Frequency dependence of the electrochemical activity contrast in AC-SECM and AFM-AC-SECM imaging

ARTICLE *in* ANALYTICAL CHEMISTRY · JANUARY 2007

Impact Factor: 5.64

READS

34

5 AUTHORS, INCLUDING:

Kathrin Eckhard

Hydro Aluminium

23 PUBLICATIONS **535** CITATIONS

SEE PROFILE

Christine Kranz

Universität Ulm

130 PUBLICATIONS **2,448** CITATIONS

SEE PROFILE

Boris Mizaikoff

Universität Ulm

310 PUBLICATIONS **4,799** CITATIONS

SEE PROFILE

Anal. Chem. **2007,** *79,* 5435−5438

Frequency Dependence of the Electrochemical Activity Contrast in AC-Scanning Electrochemical Microscopy and Atomic Force Microscopy-AC-Scanning Electrochemical Microscopy Imaging

Kathrin Eckhard,[†] Christine Kranz,[‡] Heungjoo Shin,[‡] Boris Mizaikoff,[‡] and Wolfgang Schuhmann*,[†]

Analytische Chemie—Elektroanalytik und Sensorik, Ruhr-Universität Bochum, D-44780 Bochum, Germany, and School of Chemistry and Biochemistry, Georgia Institute of Technology, Atlanta, Georgia 30306

Alternating current mode scanning electrochemical microscopy (AC-SECM) enables local detection of electrochemical surface activity without any redox mediator present in solution. *Z*-approach curves toward the substrate result in a negative feedback curve of the ac signal for insulating samples. On conducting samples, however, the shape of the feedback curve was found to be dependent on the ac perturbation frequency. Approach curves over a wide range of frequencies were performed, and the results were applied to interpret laterally resolved frequency-dependent measurements obtained with combined atomic force microscopy-AC-SECM (AFM-AC-SECM). For the first time, this frequency dependence of the signal was utilized to fine-tune the electrochemical contrast in lateral imaging in AC-SECM. An array of gold microelectrodes embedded in silicon nitride displaying significant changes in electrochemical activity as well as in topography was investigated using a bifunctional AFM-SECM tip with an integrated recessed ring microelectrode. Due to the unique geometrical conditions the electrochemical contrast between the conducting gold spots and the insulating Si_xN_y is reversed, crosses zero, and inverts as a function of the applied ac frequency.

Electrochemical impedance spectroscopy is ubiquitous in the analysis of corrosion phenomena.[1] However, the global impedance of a sample surface does not necessarily reflect processes which distribute inhomogeneously over a surface. Hence, global impedance spectroscopy is not applicable for the localized investigation of electrochemical phenomena, such as localized corrosion or the onset of the formation of corroding pits. In order to overcome this obstacle, there has been an increasing effort in developing a number of scanning electrochemical techniques.[2−5] Among those, alternating current scanning electrochemical microscopy (AC-SECM) has evolved into a powerful tool, since it bears the intrinsic advantage of mapping local surface activity without adding any redox mediator to the electrolyte solution.[6] The concept of a variation in impedance upon approaching an ultramicroelectrode (UME) to the sample surface had first been used for tip positioning.[7,8] Later it was employed as a distance control device in combination with faradaic SECM measurements.[9] In contrast to earlier observations[10] the impedimetric distance control is only applicable on electrochemically homogeneous substrates, since the signal in close proximity of the sample is dependent on the electrochemical nature of the sample. This effect has been successfully utilized in AC-SECM and has emerged into numerous applications.[6,9,11−13] Also, resistance studies of porous membranes were successfully carried out.[14,15] AC-SECM has been combined with recent instrumental improvements in SECM such as shear force mode distance regulation[16,17] and atomic force microscopy

* Author to whom correspondence should be addressed. Fax: +49 234 32-14683. Phone: +49 234 32-26200. E-mail: wolfgang.schuhmann@rub.de.

[†] Ruhr-Universität Bochum.

[‡] Georgia Institute of Technology.

(1) MacDonald, J. R. E. *Impedance Spectroscopy*; MacDonald, J. R. E., Ed.; Wiley: New York, 1987; Vol. 224.

(2) Lillard, R. S.; Moran, P. J.; Isaacs, H. S. *J. Electrochem. Soc.* **1992**, *139* (4), 1007−1012.

(3) Stratmann, M.; Streckel, H. *Corros. Sci.* **1990**, *30* (6−7), 681−96.

(4) Bard, A. J.; Fan, F. R. F.; Kwak, J.; Lev, O. *Anal. Chem.* **1989**, *61* (2), 132−138.

(5) Bayet, E.; Huet, F.; Keddam, M.; Ogle, K.; Takenouti, H. *Mater. Sci. Forum* **1998**, *289−2*, 57−68.

(6) Katemann, B. B.; Schulte, A.; Calvo, E. J.; Koudelka-Hep, M.; Schuhmann, W. *Electrochem. Commun.* **2002**, *4* (2), 134−138.

(7) Horrocks, B. R.; Schmidtke, D.; Heller, A.; Bard, A. J. *Anal. Chem.* **1993**, *65* (24), 3605−3614.

(8) Kashyap, R.; Gratzl, K. *Anal. Chem.* **1999**, *71* (14), 2814−2820.

(9) Kurulugama, R. T.; Wipf, D. O.; Takacs, S. A.; Pongmayteegul, S.; Garris, P. A.; Baur, J. E. *Anal. Chem.* **2005**, *77* (4), 1111−1117.

(10) Alpuche-Aviles, M. A.; Wipf, D. *Anal. Chem.* **2001**, *73* (20), 4873−4881.

(11) Katemann, B. B.; Inchauspe, C. G.; Castro, P. A.; Schulte, A.; Calvo, E. J.; Schuhmann, W. *Electrochim. Acta* **2003**, *48* (9), 1115−1121.

(12) Schulte, A.; Belger, S.; Etienne, M.; Schuhmann, W. *Mater. Sci. Eng., A* **2004**, *378* (1−2), 523−526.

(13) Gabrielli, C.; Huet, F.; Keddam, M.; Rousseau, P.; Vivier, V. *J. Phys. Chem. B* **2004**, *108* (31), 11620−11626.

(14) Ervin, E. N.; White, H. S.; Baker, L. A. *Anal. Chem.* **2005**, *77* (17), 5564−5569.

(15) Hirata, Y.; Yabuki, S.; Mizutani, F. *Bioelectrochemistry* **2004**, *63* (1−2), 217−224.

(16) Etienne, M.; Schulte, A.; Schuhmann, W. *Electrochem. Commun.* **2004**, *6* (3), 288−293.

(17) Eckhard, K.; Etienne, M.; Schulte, A.; Schuhmann W. *Electrochem. Commun.* **2007**, *9*, 1793−1797.

10.1021/ac070605e CCC: $37.00
Published on Web 06/14/2007

scanning electrochemical microscopy (AFM-SECM).[18] Contact mode AFM in air using a conductive tip (cAFM) has also been used to record local frequency spectra of the solid/solid interface between tip and sample.[19−21] Mapping local electrochemical properties at the solid/liquid interface simultaneously with imaging topographical information can be achieved by combined AFM-SECM.[22−25] With tip-integrated recessed ring microelectrodes, the simultaneously obtained electrochemical data is not distorted by degradation of the electrode surface even in contact mode AFM.[26−29]

In this contribution AFM-AC-SECM is used to investigate the dependency of the electrochemical contrast on the perturbation frequency. It has been reported that AC-SECM approach curves toward conducting substrate can result in either positive feedback or negative feedback response depending on the applied frequency.[30,31] To the best of our knowledge, this aspect has never been utilized for tuning the electrochemical contrast in AC-SECM imaging.

EXPERIMENTAL SECTION

Approach Curves in AC-SECM. A three-electrode arrangement was used consisting of an ultramicroelectrode, a large, ring-shaped Pt counter electrode, and a miniaturized double-junction reference electrode. The inner compartment of the reference electrode was filled with 1 M KCl, whereas the outer compartment contained 50 mM KCl to reduce the osmotic pressure on both junctions and to avoid leakage of ions into the solution of 1 mM KCl inside the electrochemical cell. Microelectrodes were prepared following a protocol described in detail before.[32] The potential applied by a potentiostat (PG 100, Jaissle Elektronik GmbH, Waiblingen, Germany) is superimposed by a sine wave specified at a lock-in amplifier (5210 Signal Recovery, Oak Ridge, TN). The resulting alternating current response is fed back from the potentiostat into the signal channel of the LIA. The phase-sensitive detection delivers the magnitude of the current as an analogue signal and is recorded via a PC as a function of the tip position. An AD-card CIO-DAS-1602/16 (Plug-In, Eichenau, Germany) and an $x-y-z$ stepper motor positioning stage (OWIS, Staufen, Germany) are used.

Combined AFM-AC-SECM. Details on the combined setup for AFM-AC-SECM measurements have been described earlier.[18] A silver/silver chloride wire serves as pseudoreference electrode (AgQRE), and a Pt-wire serves as counter electrode. The fabrication process of the AFM tip with integrated electrode has been described in detail elsewhere.[24,29] The tip-integrated ring microelectrode used in all measurements presented within this contribution had an outer radius b of 1.25 μm and an inner radius a of 1.35 μm (ratio $a/b = 0.80$). The electrode was recessed 1.05 μm from the apex of the SiC AFM tip.

RESULTS AND DISCUSSION

AC-SECM visualizes conducting and nonconducting features at the sample surface. This ability originates in a change in current distribution when the UME is placed in close proximity to a conducting site at the surface, which the current can pass through. Thereby, it bypasses the high-impedance region between tip and substrate leading to an increase in current magnitude at the tip. Since the signal is an alternating current, no charge transfer is involved and the electric field lines pass through the conductor in order to shortcut the way to the counter electrode. This possibility of an alternative pathway for the electrical field lines of lower impedance is the reason that the obtained current signal at conducting areas of the sample surface is always higher than over insulating material. Despite this fact, there are significant differences in the approach curves toward a conductive surface depending on the applied ac frequency. Approach curves toward insulating surfaces invariably result in a negative feedback response as shown for three exemplary frequencies in Figure 1A. Toward conducting surfaces, however, the shape of the approach curve can vary from negative[10] response, which is always less negative than over an insulator,[16,30,31] to positive feedback response.[6,7,13,30,31] Approach curves demonstrating this behavior of the ac current magnitude are shown in Figure 1B. For frequencies which are high with respect to the time constant of the equivalent circuit of the electrochemical cell, the response changes to positive feedback. A large contribution of the capacitive components to the overall cell impedance, i.e., low frequencies, results in a negative feedback response.[31] At the given circumstances a perturbation frequency of 1.6 kHz led to a negative feedback response, whereas 47 kHz resulted in positive feedback. The point of zero-crossing was observed at about 8 kHz. Hence, by tuning the frequency this increase in relative change of the signal can be used to obtain a significantly improved contrast in imaging of the electroactive properties at the sample surface.

While the frequency dependency of the approach curves was described previously[31] no lateral imaging had been demonstrated as a function of frequency. The influence of the frequency on the imaging contrast was investigated using combined AFM-SECM at a model sample. A periodic array of recessed gold microelectrodes of 1 μm diameter, fabricated from a gold-coated silicon wafer with a microstructured silicon nitride film (periodicity: 4 μm), was scanned in contact mode AFM-AC-SECM with a tip-integrated Pt-ring electrode. Figure 2 shows the simultaneously obtained topographical and ac image of a 25 μm × 25 μm scan recorded at a frequency of 5.01 kHz. The topographic AFM image (left) clearly shows the pore array with the expected periodicity

(18) Eckhard, K.; Schuhmann, W.; Shin, H.; Mizaikoff, B.; Kranz, C. *Electrochem. Commun.* **2007**, *9*, 1311−1315.
(19) Shao, R.; Bonnell, D. A. *Jpn. J. Appl. Phys., Part 1* **2004**, *43* (7b), 4471−4476.
(20) O'Hayre, R.; Lee, M.; Prinz, F. B. *J. Appl. Phys.* **2004**, *95* (12), 8382−8392.
(21) Pingree, L. S. C.; Hersam, M. C. *Appl. Phys. Lett.* **2005**, *87* (23), Art. No. 233117.
(22) Macpherson, J. V.; Unwin, P. R. *Anal. Chem.* **2001**, *73*, 550.
(23) Kranz, C.; Friedbacher, G.; Mizaikoff, B.; Lugstein, A.; Smoliner, J.; Bertagnolli, E. *Anal. Chem.* **2001**, *73* (11), 2491.
(24) Lugstein, A.; Bertagnolli, E.; Kranz, C.; Mizaikoff, B. *Surf. Interface Anal.* **2002**, *33* (2), 146−150.
(25) Dobson, P. S.; Weaver, J. M. R.; Holder, M. N.; Unwin, P. R.; Macpherson, J. V. *Anal. Chem.* **2005**, *77* (2), 424−434.
(26) Lugstein, A.; Bertagnolli, E.; Kranz, C.; Kueng, A.; Mizaikoff, B. *Appl. Phys. Lett.* **2002**, *81* (2), 349−351.
(27) Kueng, A.; Kranz, C.; Mizaikoff, B.; Lugstein, A.; Bertagnolli, E. *Appl. Phys. Lett.* **2003**, *82* (10), 1592−1594.
(28) Kranz, C.; Kueng, A.; Lugstein, A.; Bertagnolli, E.; Mizaikoff, B. *Ultramicroscopy* **2004**, *100* (3−4), 127−134.
(29) Shin, H.; Hesketh, P.; Kranz, C.; Douglas, D. R.; Mizaikoff, B. *Proc. ASME* **2007**, *79*, 4769−4777.
(30) Baranski, A. S.; Diakowski, P. M. *J. Solid State Electrochem.* **2004**, *8* (10), 683−692.
(31) Diakowski, P. M.; Baranski, A. S. *Electrochim. Acta* **2006**, *52* (3), 854−862.
(32) Kranz, C.; Ludwig, M.; Gaub, H. E.; Schuhmann, W. *Adv. Mater.* **1995**, *7* (6), 568−571.

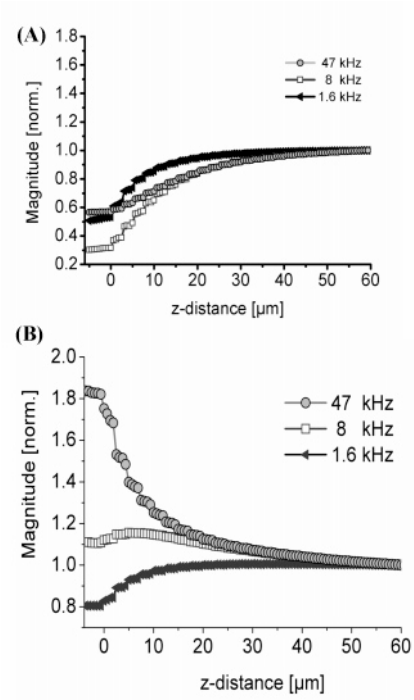

Figure 1. AC-SECM approach curves on SiO_2 (A) and Au (B). Displayed is the current magnitude vs *z*-distance. The sharp bend in the electrochemical signal indicates the electrode touching the surface and serves as zero-distance. $d_{tip} = 10\ \mu m$, 1 mM $KClO_4$, $V_{pp} = 100$ mV, $f = 1.6$, 8, and 47 kHz.

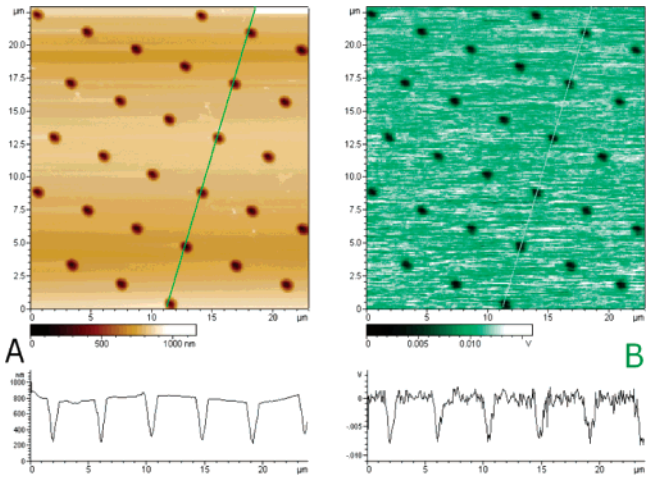

Figure 2. Simultaneously recorded contact mode AFM (left) image and AC-SECM image (right); scan area 25 μm × 25 μm, $c = 1$ mM KCl, $V_{pp} = 110$ mV, $f = 5.01$ kHz.

of 4 μm. The length of the thorn of the combined AFM-SECM tip defines the small gap between microring electrode and substrate. Hence, a thin film electrolyte is created where the current has to pass through leading to an increased impedance between working (tip) and counter electrode. Since the recessed underlying gold substrate is large, the high impedance of the thin film electrolyte can be avoided by electric field lines taking a path into the gold layer, traveling laterally with almost no impedance, and leaving the conducting substrate at a remote place closer to the counter electrode. The recessed gold microspots are interconnected offering a shortcut for the ac current. Hence, the current magnitude at these sites is expected to increase. However, the

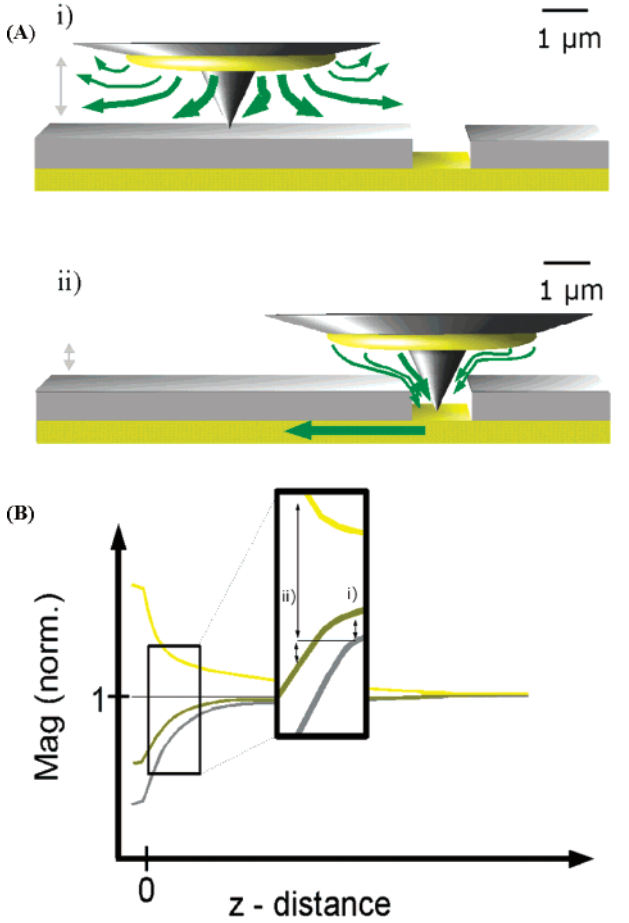

Figure 3. (A) Schematic close-up on the integrated tip electrode and the sample. Distances are to scale. (B) Schematic representation of AC-SECM approach curves toward an insulating surface (gray), toward a conductor at low perturbation frequency (dark yellow), and toward a conductor at high perturbation frequency (bright yellow). The inset shows the signal change upon variations in the sample conductivity along with the probe-to-sample distance; i and ii refer to the conditions shown in part A of the figure.

AC-SECM image in Figure 2 indicates a decreased value in current magnitude above the gold spots in comparison to the value obtained over silicon nitride.

The reason for this result can be explained by the geometric particularities of the probe and surface structure. AFM-SECM is a combined technique providing superior topographic resolution leading to a constant distance between the integrated electrode and a flat sample surface. However, if topological surface features are comparable in size to the length of the thorn of the AFM tip, a change in electrode-to-sample distance has to be taken into account. The sketch to scale shown in Figure 3Ai illustrates the investigated model sample in relation to the tip-integrated electrode. The recessed ring electrode (diameter 2.7 μm) has about 2.7 times the diameter of the recessed gold spot. When the AFM thorn travels into the pore, this leads to a significant decrease in the ring electrode-to-sample distance (Figure 3Aii). Therefore, the impedance is increased due to the decrease of the electrolyte film thickness.

Independently of the shape of the approach curve the signal of the current magnitude should always increase when the electrode scans from a nonconducting to a conducting part of the sample (Figure 3B). Interestingly, the expected signal increase

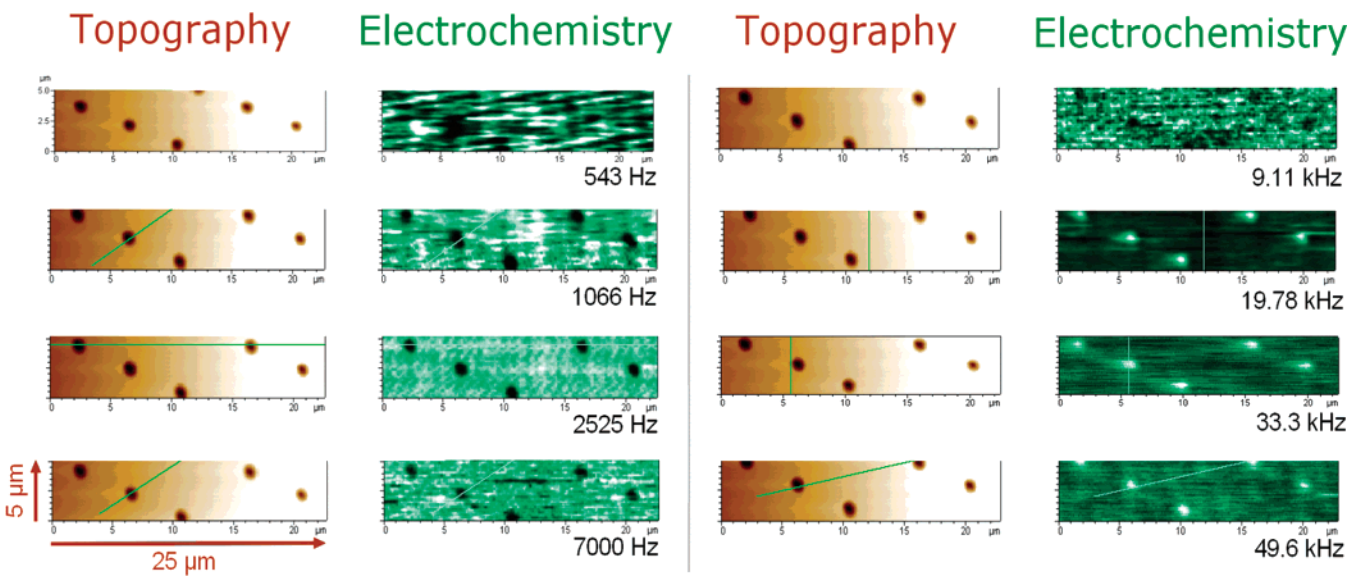

Figure 4. Series of AFM-AC-SECM measurements at different perturbation frequencies. Corresponding topographic information is on the left, and electrochemical information is on the right. $c = 1$ mM KCl, $V_{pp} = 110$ mV; perturbation frequency is as indicated.

can be masked, if a change in distance occurs simultaneously. The electroactive area of the combined AFM-SECM probe is 450 nm closer (thickness of the insulating layer of the sample) to the Si_xN_y surface when the thorn moves into the pore. The local impedance increases due to the smaller electrolyte film thickness in the gap. This leads to a value of the current magnitude correlated to a point of the approach curve, which is closer to the surface and, hence, results in a smaller signal as long as the chosen frequency causes a negative feedback above the conductor.

Since the slope of the approach curve is dependent on the ac frequency applied (see Figure 1), the image contrast should change as positive feedback is obtained at sufficiently high frequency due to a suppressed contribution of capacitive components to the overall cell impedance. In the case of positive feedback the signal of the current magnitude over a conducting site is higher than over an insulator regardless of any changes in distance. This frequency dependence of the contrast was further investigated in a series of scans with perturbation frequencies ranging from 543 Hz to 49.6 kHz. As can be derived from Figure 4, there obviously is a threshold frequency where AC-SECM imaging is possible. Perturbation frequencies of 543 Hz and below do not lead to sufficient electrochemical sensitivity. The images recorded at 1066, 2525, and 7000 Hz are similar to the image shown in Figure 2 with the scan at 2525 Hz providing the highest electrochemical contrast in the left-hand column. The AC-SECM images in the right-hand column show the inversion at higher frequencies (19.78, 33.3, and 49.6 kHz) that is caused by a switch to positive feedback in the approach curves over conductive substrates at higher frequencies as shown in Figure 1. The signal-to-noise ratio in this specific experimental setup decreased with higher frequencies most probably due to limitations caused by the bandwidth of the employed potentiostat. The expected zero-crossing of the contrast was obtained at 9.11 kHz in the AFM-AC-SECM imaging series. An upper limit of the perturbation frequency was not determined in this set of experiments.

CONCLUSION

Visualizing confined conducting spots within an insulating matrix can serve as a simplified model for identifying precursor sites for pitting corrosion. For the first time the dependence of the lateral electrochemical contrast on the ac frequency is shown in a sequential series of scans. The presented results suggest the frequency along with the topography is crucial to avoid misinterpretation of data (see Figure 4 at 9.11 kHz), especially over unknown samples. Hence, the determination of the absolute distance of the electrode to sample together with the tip geometry is essential for AC-SECM studies of unknown samples. Future work will focus on automation of the frequency changes during ac scanning recording a full admittance spectra at each point in space.

ACKNOWLEDGMENT

These studies were partially supported by the DAAD—German Academic Exchange Board (K.E., W.S.). B.M. and C.K. acknowledge support by the NSF within the program "Biocomplexity in the Environment" (No. 0216368). Furthermore, the FIB^2 Center and the MiRC facility at Georgia Institute of Technology are acknowledged.

Received for review March 27, 2007. Accepted May 9, 2007.

AC070605E